Strathprints Institutional Repository

Proceedings of the ASME 2010 29th International Conference on Ocean, Offshore and Arctic Engineering
OMAE2010
June 6-11, 2010, Shanghai, China

OMAE2010-20192

NUMERICAL AND EXPERIMENTAL COMPARISONS OF VORTEX-INDUCED VIBRATIONS OF MARINE RISERS IN UNIFORM/SHEARED CURRENTS

Narakorn Srinil *
Department of Naval Architecture & Marine Engineering
University of Strathclyde, Glasgow
Scotland, UK

Patrick O'Brien
MCS Kenny
Aberdeen
Scotland, UK

Marian Wiercigroch
School of Engineering, King's College
University of Aberdeen
Scotland, UK

ABSTRACT

This paper presents a general theoretical reduced-order model capable of evaluating the *multi-mode* nonlinear dynamics of marine risers subject to *uniform* and *sheared* currents. The main objectives are to predict the vortex-induced vibration responses and parametrically compare between numerical and experimental results. The emphasis is placed on the analysis of *cross-flow* vibrations due to unsteady lift forces.

The nonlinear equations governing riser axial/transversal motions are derived based on a top-tensioned beam model with typical pinned-pinned boundary conditions. The riser geometric nonlinearities owing to possible large dynamic displacements and multi-mode interactions are accounted for. To approximate the *space-time* varying lift force, the empirical hydrodynamic model, based on a nonlinear van der Pol wake oscillator with a distributed diffusive term, is used. A low-dimensional dynamic model and computationally-robust time-domain tool are then developed to evaluate the multi-mode fluid-riser interactions. These are very useful in dealing with large parametric studies involving varying system parameters.

Comparisons of numerical and experimental results are performed by estimating riser response amplitudes and fatigue damage indices. Both linear and nonlinear risers are considered in the present numerical model whereas only linear riser has been considered by a referenced literature in the reconstruction of experimental displacements through measured strains. It is found that riser *geometric nonlinearities* play a significant role in both numerical simulations and comparisons with experiment post-processed results. In some cases, quantitative/qualitative discrepancies in riser response predictions are remarkable with linear vs. nonlinear models. These may be recognized as one of the factors why recent numerical and experimental comparisons in literature have been unsuccessful.

1. INTRODUCTION

Vortex-induced vibrations (VIV) of marine risers exhibit intriguing fluid-solid interaction phenomena in ocean science and engineering applications. When exposed to current flows, these cylindrical bodies undergo nonlinear oscillations owing to the space-time varying hydrodynamic forces associated with vortex shedding. Because VIV result in both the increased mean drag and high fatigue damage in long flexible structures, they are ones of the utmost concerns in deepwater developments. In general, the VIV fatigue accumulation depends on a number of mechanical, physical and fluid-solid parameters, apart from being a function of modal characteristics including modes, frequencies, amplitudes and curvatures. Based on the Strouhal rule relating the vortex-shedding frequency to flow velocity [1], different modes are potentially excited and nonlinearly interact in a distributed-parameter or infinite-dimensional system. To understand a wide variety of dynamic scenarios induced by overall hydrodynamics and geometric nonlinearities, a computationally-robust fluid-riser interaction model and systematic analytical/numerical approach – which account for experimental observations as many as feasible – are needed.

Recently, some new experimental measurements of large-scale risers in field currents and laboratory fluid flows have provided benchmark data meaningful for validations of the empirical-based formulations and prediction tools for riser VIV. However, many insights into nonlinear dynamics of such flexible cylinders subject to VIV are still far from fully understood. These include, for instance, the description of space-time sharing, switching and interaction of modes in different lock-in or synchronization regimes [2], the standing vs. travelling wave characteristics of risers in sheared flows [3], the dependence of Reynolds number [4], the influence of initial curvatures of inclined cylinders [5], the importance of

*corresponding author: narakorn.srinil@strath.ac.uk

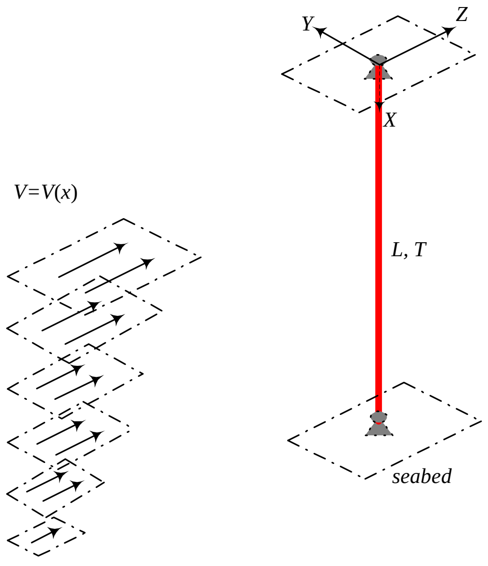

Figure 1 Schematic model of riser subject to a linearly sheared flow

geometric nonlinearities [2], mode order and higher harmonics [6], the non-periodic, non-resonant and chaotic responses [7]. Indeed, through lack of realistic theoretical models capable of capturing the aforesaid aspects, large discrepancies still occur in recent VIV prediction comparisons by the most common industrial codes and experiments [8]. It is worth mentioning that, based on a typical post-processing analysis of experiment data in frequency domain with a linear modal approach, the significance of multi-mode contributions and nonlinear interactions during the VIV might have been disregarded through the measured strain- or acceleration-based displacement calculations. Therefore, a more realistic data post-processing technique or a robust time-domain predictive tool which accounts for overall nonlinear effects as well as multi-mode interaction features is needed.

This paper aims to develop and improve a reduced-order hydrodynamics-riser interaction model capable of describing the multi-mode nonlinear dynamics and interactions of risers undergoing VIV. Top-tensioned risers in both uniform and linearly sheared currents are considered and comparatively discussed. Based on some available hydrodynamic coefficients of lift forces acting on cylinders, only cross-flow VIV are herein investigated. Within a numerical time-domain framework, attention is placed on qualitatively and quantitatively describing the multi-mode interaction characteristics in space and time, and comparing between numerical and experimental results. To this end, riser experiments investigated by ExxonMobil are considered. Their post-processed results have recently been reported by Tognarelli *et al*. [9]. Our main findings will highlight the important effect of riser geometric nonlinearities and sheared flow on theoretical modeling, response predictions and comparisons of numerical and experimental studies, along with some aspects of riser VIV.

2. HYDRODYNAMICS-RISER INTERACTION MODEL

The great majority of research literature dealing with modeling and analysis of riser VIV considers a single *linear* equation of motion of straight tensioned beam subject to time-dependent hydrodynamics. To describe the fluctuating lift or drag forces associated with vortex shedding, different models and methodologies have been considered which, in general, comprise the computational fluid dynamics CFD [10], the strip theory [11] and the empirical-based approach [12]. The former two models are solved in time domain whereas the latter model is solved, with much less calculation efforts, either in frequency or time domain via energy balance or numerical integrations, respectively. Nevertheless, recent studies and comparisons with experimental measurements still reveal discrepancies in riser VIV predictions among these models and computer codes [8]. This is because neither of them can fully capture overall nonlinear dynamics and behaviors due to the space/time fluid-structure interactions which are extremely complicated in deepwater applications with arbitrary flows. With respect to riser analysis and design involving varying system parameters, the empirical approach is perhaps preferable to industry since, apart from the computational efficiency viewpoint, relevant models and system coefficients are simply revised and calibrated according to the available sets of experimental data.

Nonlinear Equations of Riser Motion and Wake Oscillator

Following Srinil *et al*. [2, 13], a reduced-order nonlinear riser/hydrodynamics interaction model, valid for arbitrarily sagged and inclined risers, is considered. Due to lack of new experimental results of curved (e.g., catenary or lazy-wave) risers, only vertical top-tensioned risers in both uniform and linearly sheared currents are analyzed and compared. As shown in Fig. 1, the modeled riser has a fully-submerged span length L, constant tension T and pinned-pinned supports. With X axis being oriented towards the sea bottom from surface, axial coordinate x being an independent spatial variable and overall displacement-related variables being normalized with respect to D, a general function describing linearly sheared flow is $V(x) = V_{max}(1-\beta x)$ where V_{max} is the maximum velocity and β is the shear parameter given by [14]

$$\beta = \frac{\Delta V}{V_{\max}}\left(\frac{D}{L}\right), \quad (1)$$

where D is the riser hydrodynamic diameter and the absolute value ΔV is the difference in velocities at the surface and seabed. Note that, in the absence of riser initial curvatures, the incoming flow direction is arbitrary such that cross-flow (in-line) VIV is aligned with Y (Z) axis by following the right-hand rule. The shear effect β depends on both the aspect ratio (L/D) and shear fraction ($\Delta V/V_{max}$). As β decreases, the correlation of vortex shedding along riser span affecting the lock-in regime is expected to increase and eventually become maximized when β = 0 in uniform flow case.

Based on the so-called engineering strain description, the nonlinear extensional dynamic strain e_d due to finite-amplitude *cross-flow* motion of riser is considered and expressed as [15]

$$e_d = u' + \frac{1}{2}\left(u'^2 + v'^2\right). \tag{2}$$

Consequently, by applying the standard variational formulation, the *nonlinear* partial-differential equations governing *coupled* axial (u) and transversal (v) motions of riser in cross-flow direction read [15]

$$\ddot{u} + \frac{c}{m+m_a}\dot{u} + \delta u'''' - \beta\left\{u'(1+\alpha) + \alpha\left(u'^2 + \frac{1}{2}\left(u'^2 + v'^2\right)\right) + \frac{\alpha}{2}\left(u'^3 + u'v'^2\right)\right\}' = 0, \tag{3}$$

$$\ddot{v} + \frac{c}{m+m_a}\dot{v} + \delta v'''' - \beta\left\{v' + \alpha u'v' + \frac{\alpha}{2}\left(u'^2 v' + v'^3\right)\right\}' = \frac{H_y}{(m+m_a)D}, \tag{4}$$

where the hydrodynamic lift force H_y entailing cross-flow VIV is expressed as [16]

$$H_y = \frac{1}{2}\rho D V^2 C_L = \frac{1}{2}\rho D V^2\left(Q - 2\gamma\dot{v}/\omega_s\right). \tag{5}$$

Herein, a prime (overdot) denotes differentiation with respect to x (t). The mechanical parameters are the viscous damping coefficient c, $\delta = EI/(m+m_a)D^4$, $\beta = T/(m+m_a)D^2$, $\alpha = EA_r/T$, in which m is the riser mass (including contents), m_a the fluid added mass, EI and EA_r the bending and axial stiffness, respectively. The fluid properties include the density ρ, lift coefficient C_L, stall parameter γ and vortex frequency ω_s (rad/s). By assuming that a Strouhal number (St) is constant, $\omega_s(x) = 2\pi \mathrm{St} V(x)/D$. The second expression in Eq.(5) has been introduced by Skop and Balasubramanian [16] to account for the fluctuation of lift coefficient. By following the extended study on sheared flows by Balasubramanian *et al*. [17], the empirical wake variable Q in Eq.(5) is governed by the following van der Pol *diffusive* wake oscillator

$$\ddot{Q} - \omega_s G\left(C_{L0}^2 - 4Q^2\right)\dot{Q} + \omega_s^2 Q - \tau\dot{Q}'' = \omega_s F\dot{v}, \tag{6}$$

where C_{L0} is the lift coefficient of fixed cylinder, F and G are the scaling wake coefficients, and τ is the diffusion parameter which is given, based on a few experimental results, by [17]

$$\tau = 0.013\left(L/D\right)^2 \omega_{s,\max}\beta. \tag{7}$$

This diffusive term has been introduced in an attempt to capture the cellular vortex-shedding feature due to sheared flow. Another diffusive wake oscillator model similar to Eq. (6) has also been presented by Mathelin and Langre [18]. The coupled Q and v are space-time dependent. Based on the flow profile, $\omega_s(x) = \omega_{s,max}(1-\beta x)$ in which $\omega_{s,max}$ is the maximum vortex frequency. Depending on system parameters, F and G may be spatially fixed or variable with varying V or Reynolds (Re) number [2]. In the latter case, the functions of $F(x)$ and $G(x)$ are determined *a priori*. This aspect will be discussed in Section 3 through the parametric investigations.

Reduced-Order System for Multi-Mode VIV Analysis

Towards the aim of predicting the riser cross-flow VIV responses and associated nonlinear dynamic behaviors due to uniform and sheared flows, a general reduced-order system which solves for a few degrees of freedom is developed. The approach is computationally efficient as opposed to the finite element- or CFD-based models. To make a comparison of obtained numerical results with published experimental data which have mostly been post-processed, regardless of flow conditions, via a linear modal analysis, the standing wave characteristics are herein assumed in the time-domain solution. Note that some recent riser experiments at high-mode VIV have observed travelling wave responses with regard to sheared flows [3]. Nevertheless, due to lack of relevant theoretical model and explanation, it is unclear whether the complexity in sheared-flow responses is due to the intrinsic behavior, the superimposition of individual standing-wave eigenmodes or both of them [19]. Therefore, our emphasis is placed on discussing the standing-wave responses due to uniform/sheared currents. In so doing, Eqs. (3)-(4) are first rearranged in the state-space or first-order forms and then projected onto an infinite-dimensional eigenbasis through riser/wake displacement and velocity variables as follows.

For riser dynamics,

$$\begin{aligned} \dot{u} = A_1 \rightarrow \quad u(x,t) &= \sum_{n=1}^{\infty}\phi_n(x) f_n(t), \quad & A_1(x,t) &= \sum_{n=1}^{\infty}\phi_n(x) p_n(t), \\ \dot{v} = A_2 \rightarrow \quad v(x,t) &= \sum_{n=1}^{\infty}\varphi_n(x) f_n(t), \quad & A_2(x,t) &= \sum_{n=1}^{\infty}\varphi_n(x) p_n(t). \end{aligned} \tag{8}$$

For wake dynamics,

$$\dot{Q} = B \rightarrow \quad Q(x,t) = \sum_{n=1}^{\infty}\varphi_n(x) d_n(t), \quad B(x,t) = \sum_{n=1}^{\infty}\varphi_n(x) e_n(t). \tag{9}$$

where ϕ_n and φ_n are axial and transversal mode shape functions associated with natural frequencies ω_n of the submerged riser. These have been obtained based on a Fourier sine series and a hybrid analytical/numerical solution of linear free undamped equations of motion in (3)-(4) with bending/extensibility effect [13]. In Eqs. (8)-(9), f_n (d_n), p_n (e_n) are generalized coordinates of riser (wake) to be determined. By substituting Eqs.(8)-(9) into (3)-(6), performing the Galerkin procedure with zero displacements and curvatures at end boundaries, applying the orthonormalization of modes and enforcing the multi-mode resonant conditions ($\omega_{s,max} \approx \omega_n$), a reduced-order system governing riser/wake interactions reads

$$\dot{f}_n = p_n, \quad (10)$$

$$\dot{p}_n = -2\xi_n\omega_n p_n - \omega_n^2 f_n + \mu\omega_n^2 \sum_{i=1}^{\infty}\left[\int_0^{L/D}\phi_n(x)(1-\beta x)^2\phi_i(x)\,dx\right]d_i - 2\mu\gamma\omega_n \sum_{i=1}^{\infty}\left[\int_0^{L/D}\phi_n(x)(1-\beta x)\phi_i(x)\,dx\right]p_i + \sum_{i=1}^{\infty}\sum_{j=1}^{\infty}\Lambda_{nij} f_i f_j + \sum_{i=1}^{\infty}\sum_{j=1}^{\infty}\sum_{k=1}^{\infty}\Gamma_{nijk} f_i f_j f_k, \quad (11)$$

$$\dot{d}_n = e_n, \quad (12)$$

$$\dot{e}_n = C_{L0}^2\omega_n \int_0^{L/D}\phi_n(x)(1-\beta x)G(x)\phi_n(x)\,dx e_n - 4\omega_n \int_0^{L/D}(1-\beta x)G(x)\phi_n^4(x)\,dx e_n d_n^2 - \omega_{s,\max}^2 \int_0^{L/D}(1-\beta x)^2\phi_n^2(x)\,dx d_n + \tau\int_0^{L/D}\phi_n(x)\phi_n''(x)\,dx e_n + \omega_n \int_0^{L/D}(1-\beta x)F(x)\phi_n^2(x)\,dx p_n + \sum_{i=1, i\neq n}^{\infty}\left[C_{L0}^2\omega_n \int_0^{L/D}\phi_n(x)(1-\beta x)G(x)\phi_i(x)\,dx e_i - \omega_{s,\max}^2 \int_0^{L/D}(1-\beta x)^2\phi_n(x)\phi_i(x)\,dx d_i + \tau\int_0^{L/D}\phi_n(x)\phi_i''(x)\,dx e_i + \omega_n\int_0^{L/D}(1-\beta x)F(x)\phi_n(x)\phi_i(x)\,dx p_i\right] - 4\omega_n \sum_{i=1, i\neq n}^{\infty}\sum_{j=1, j\neq n}^{\infty}\sum_{k=1, k\neq n}^{\infty}\int_0^{L/D}(1-\beta x)G(x)\phi_n(x)\phi_i(x)\phi_j(x)\phi_k(x)\,dx d_i d_j e_k. \quad (13)$$

The multi-mode interaction coefficients associated with riser geometric nonlinearities are given by

$$\Lambda_{nij} = -\beta\alpha\int_0^{L/D}\left(\frac{3}{2}\phi_n'\phi_i'\phi_j' + \frac{1}{2}\phi_n'\varphi_i'\varphi_j' + \varphi_n'\phi_i'\varphi_j'\right)dx, \quad (14)$$

$$\Gamma_{nijk} = -\frac{\beta\alpha}{2}\int_0^{L/D}\left(\phi_n'\phi_i'\phi_j'\phi_k' + \phi_n'\phi_i'\varphi_j'\varphi_k' + \varphi_n'\varphi_i'\phi_j'\phi_k' + \varphi_n'\varphi_i'\varphi_j'\varphi_k'\right)dx. \quad (15)$$

Note that Eq. (14) is trivial when only transverse modes are accounted for in the riser VIV analysis. Yet, depending on riser elasticity (E), the axial mode contributions and interactions with transverse modes through Eqs.(14)-(15) may be significant, and these should not be ruled out. The tuning of vortex ($\omega_{s,max}$) and natural (ω_n) frequencies is also accounted for through Eq.(13). ξ_n is the modal damping ratio, assumed to be equal for all eigenmodes ($\xi_n \approx \xi$). This entails a unique mass-damping (so-called Skop-Griffin) parameter defined by $S_G = \xi/\mu$, where the relevant mass ratio is $\mu = \rho D^2/8\pi^2 St^2(m+m_a)$ [16]. If the effects of longitudinal motion, inertia and geometric nonlinearities are neglected, Eq. (4) reduces to the linear equation of tensioned beam which is widely used in literature. Overall, the $4N$ Eqs. (10)-(13) are simultaneously solved by a numerical integration method with stable time stepping and properly-assigned initial conditions of displacements and velocities.

3. MULTI-MODE DYNAMICS AND INTERACTIONS IN RISER VIV: UNIFORM/SHEARED CURRENTS

This study aims to numerically investigate the multi-mode dynamics and interactions in nonlinear riser VIV due to uniform and sheared currents. To capture different dynamic scenarios, the flow velocity V (or ω_s) is parametrically varied in the analysis. In sheared flow cases, the maximum/minimum flow velocities (V_{max}/V_{min}) are both varied such that β remains constant. By way of examples, the tested ExxonMobil riser is considered [9] whose properties and fluid-structure parameters are summarized in Table 1 below.

Table 1 Riser properties and parameters

	Value	Unit
L	9.63	m
D	20	mm
T	700	N
E	1.025x10^{11}	N/m^2
ρ	1000	kg/m^3
V_{max}	0.1-2.5	m/s
V_{min}	0.14V_{max}	m/s
Re$_{max}$	0.4x10^5	-
ξ	0.003	-
μ	0.173	-
St	0.17	-
γ	0.183	-
F	0.319*	-
G	1.887*	-
CL_0	0.28	-
β	0.0018	-

* based on S_G = 0.0173 [13, 16]

As aforesaid, the values of wake parameters F and G may be altered with varying V by also accounting for the Re number effect in the empirical derivation [2]. In sheared flow cases, both functions $F(x)$ and $G(x)$ are determined *a priori*, but this is not straightforward in varying many V_{max} (V_{min}) cases since the integrals governing overall modal coefficients in Eq.(13) have to be recalculated every time. To avoid such time-consuming task, $F(x)$ and $G(x)$ based on V_{max} = 2.5 m/s are evaluated and assumed in all cases. In so doing, the analysis starts by computing F and G values at 51 nodes along riser from x = 0 to $x = L/D$ (481.5). It is found that $F(x)$ is nearly constant such that $F(x)\approx 0.3$ whereas $G(x)$ varies from 1.38 (at the top) to 3.06 (at the bottom). Accordingly, a curve for $G(x)$ is constructed to determine the associated continuous functions by making use of polynomials with different orders. All G values are again calculated based on these functions and compared, in terms of percent differences, with those obtained at the same discrete points. With increasing order of polynomials for a convergence purpose, it is found that the 7th-order polynomials provide the percent differences being less than 1% at all nodes. Therefore, we assume a constant F=0.3 whereas $G(x)$ is described by a 7th-order polynomial function as follows

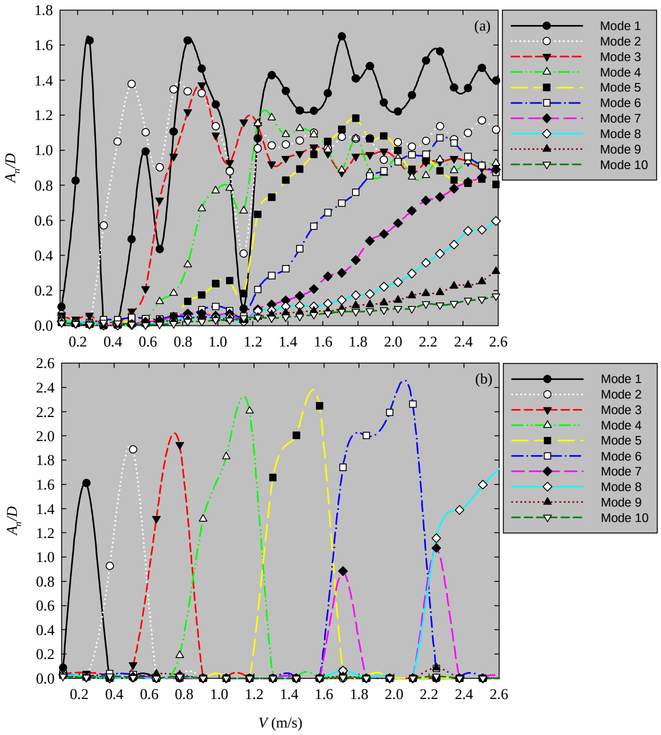

Figure 2 Variation of A_n/D with V for ExxonMobil riser in uniform current: (a) nonlinear and (b) linear riser models with N=10

$$G(x) = 6.34x10^{-18}x^7 - 9.05x10^{-15}x^6 + 5.17x10^{-12}x^5 - 1.47x10^{-9}x^4 + 2.19x10^{-7}x^3 - 1.45x10^{-5}x^2 + 1.20x10^{-3}x + 1.38. \quad (16)$$

Based on the general standing-wave solution in Eq.(8), the predicted maximum amplitude of each individual mode due to cross-flow VIV is given by

$$A_n/D = \left| f_n\left(t_{n,\max}\right)\varphi_n\left(x_{\max}\right)\right|. \quad (17)$$

For a given flow profile and entire velocity range, a number of N modes may be excited concurrently or non-concurrently. With $N = (N_2\text{-}N_1) + 1$, the space-time varying amplitudes accounting for all resonant/non-resonant modes are given by

$$v_j\left(x,t_j\right) = \sum_{n=N_1}^{N_2} f_n\left(t_j\right)\varphi_n\left(x\right). \quad (18)$$

Accordingly, the root-mean-squared (RMS) amplitude (A_{rms}/D) at a specific riser position can be determined based on Eq.(18), together with the spatially maximum value ($A_{rms,max}/D$).

Finally, the "fatigue damage index" (FDI), proportional to the riser fatigue damage, may be approximated by [9, 20]

$$\text{FDI} = f_d \varepsilon^3, \quad (19)$$

where, for simplicity, f_d is the natural frequency (Hz) of a mode predominating in VIV response and ε is the micro bending strain calculated based on the RMS riser dynamic curvature (K).

It is worth noting that the typical fatigue damage is calculated based on a ratio of the number of cycles incurred over the number of cycles to failure. This may be evaluated through the S-N curve which entails the proportionality relationship: fatigue damage $\propto f_d\sigma^3$ [21]. Since the stress σ is proportional to bending strain that can be directly measured from experiments, Tognarelli *et al.* (2004) have introduced this FDI to simply approximate the fatigue damage with a slope of 3 from S-N curve. In fact, Eq. (19) is independent of a stress concentration factor, elastic modulus or S-N curve intercept, but providing these properties would yield actual fatigue damage that is proportional to the FDI by a constant factor [9].

In the following, the multi-mode dynamics, sharing and interactions in riser VIV due to both uniform and linearly sheared flows are discussed through amplitude response diagrams and spatial displacement profiles. As typically tested in the experiments, the case of increasing V is considered with a small V increment. The mode number, as well as mode order, is also increasingly varied to achieve solution convergence [2].

Riser in Uniform Current

The case of riser in uniform current is analyzed first. To account for the flow velocity range of $0.1<V<2.6$ m/s and the convergence of solution with varying V, the first 10 riser modes are considered in the reduced-order model. The variation of wake parameters (F, G) with varying Re is also accounted for [2]. With N=10 (n=1-10), Figure 2 compares the maximum response amplitudes of individual modes contributing to riser VIV, based on nonlinear (2a) and linear (2b) riser models. It is seen that considerable quantitative/qualitative differences take place between the two response diagrams.

In Fig. 2b, the linear model exhibits a typical single-mode lock-in feature in different V ranges with jump phenomena and mode-switching of response amplitudes. The lock-in bandwidth as well as the modal response seems to increase with mode number. The overall maximum A_n/D reaches the value of 2.4. The 7th mode response reveals two small peaks and shares with the 6th and 8th mode higher-amplitude responses. The 9th and 10th modes are not excited in this V range.

On the contrary, the nonlinear model in Fig. 2a reveals the strong multi-mode dynamics and interactions throughout the V range with high/low modes being driven into the responses. The relevant time histories are quite fluctuating, depending on initial conditions. The uni-modal lock-in phenomenon appears at very low V involving the 1st mode. This mode seems to be the most energetic one for this riser. Both 9th and 10th modes are excited at high V values. Overall, the maximum A_n/D is about 1.6, which is much lower than that predicted by linear model.

By accounting for all modal contributions through Eq. (18), the 3-D plots of superimposed displacement profiles predicted by linear/nonlinear models are now comparatively displayed in Fig. 3, in terms of A_{rms}/D. "normalized x" indicates how the coordinate x has further been normalized in such a way that the spatially maximum value is equal to 1. It is seen that as V increases the linear model shows the increasing number of half-sine waves along riser span, regularly following the tensioned beam mode number. The responses are either symmetric or anti-symmetric with respect to the mid-span. In contrast, the nonlinear model eliminates the half-sine waves due to multi-mode combinations. Regarding the overall responses, the linear model overestimates the amplitudes with $A_{rms,max}/D \approx 0.70$ when compared to those by nonlinear model with $A_{rms,max}/D \approx 0.59$.

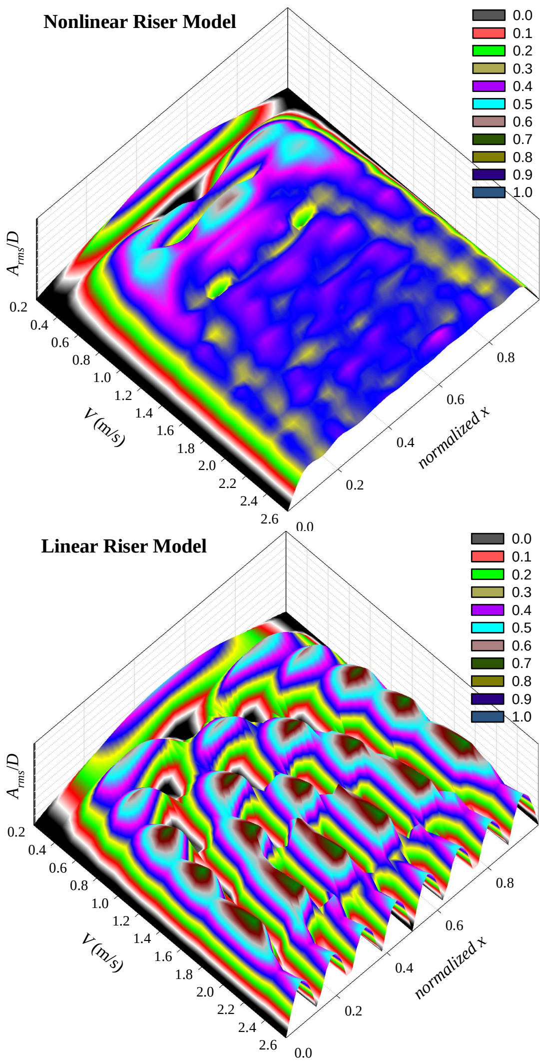

Figure 3 Space-time varying A_{rms}/D with V for ExxonMobil riser in uniform current: nonlinear vs. linear riser models with N=10

Riser in Sheared Current

The linearly sheared flow is now considered by making use of linear and/or nonlinear riser model. The values of V along riser are varied such that the shear parameter β remains constant. Recall that the wake coefficient $G = G(x)|_{V=2.5}$ whereas F is constant. Although the diffusive wake oscillator is used (Eq. 6), the location determination of cellular vortex-shedding is herein disregarded since we have performed a full-span numerical integrations in the reduced-order approximations (Eqs.10-15). This location may be realized when directly solving Eqs.(2)-(6).

With N = 9 and 23 varying V cases, the variation of modal amplitudes (A_n/D) with V_{max} are illustrated in Figs. 4a and 4b by non-linear and linear riser models, respectively. It can be seen that all the individual modal responses are considerably reduced (i.e., maximum $A_n/D < 0.30$) when compared to Figs. 2a and 3a in the uniform flow case. This trend of decreasing response amplitudes is in agreement with experimental [9] and CFD [10] results. A typical single-mode lock-in – where the response clearly shows a hysteresis effect with one major peak – is likely to occur in Figs. 4a and 4b for some modes (n = 1, 2), though being due to sheared flow [22]. Nevertheless, some other modes (e.g., n = 3, 6) reveal multiple peaks and their responses overlap in certain velocity ranges. This clearly shows the feature of multi-mode responses even with linear riser model (Fig. 4b).

Because of these small vibration amplitudes, the geometric nonlinearities play a negligible role in the amplitude prediction of riser VIV in sheared flow. The numerical results predicted by linear and nonlinear models are indeed comparable, showing minor quantitative or qualitative discrepancies. These become more apparent when superimposing all modal responses and evaluating RMS amplitudes. Yet, the nonlinear model should be considered for the sake of generality.

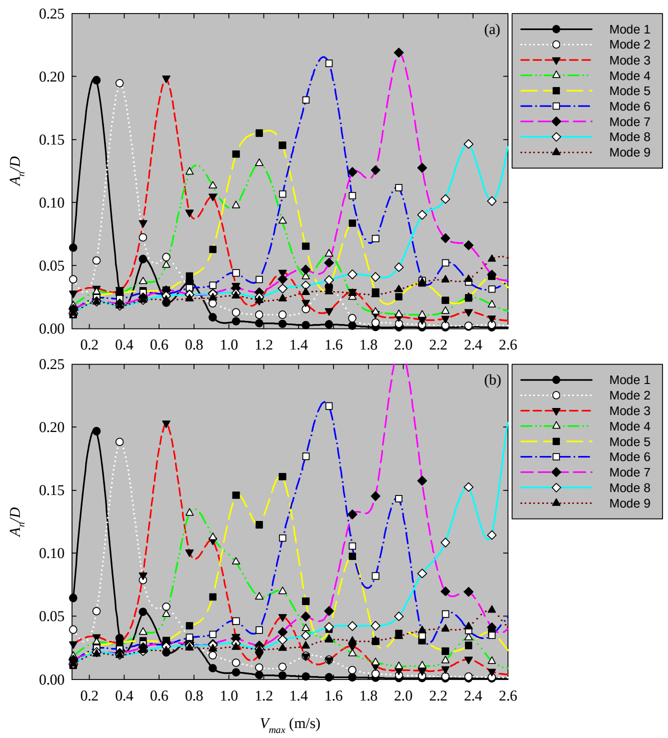

Figure 4 Variation of A_n/D with V for ExxonMobil riser in linearly sheared current: (a) nonlinear and (b) linear riser models with N=9

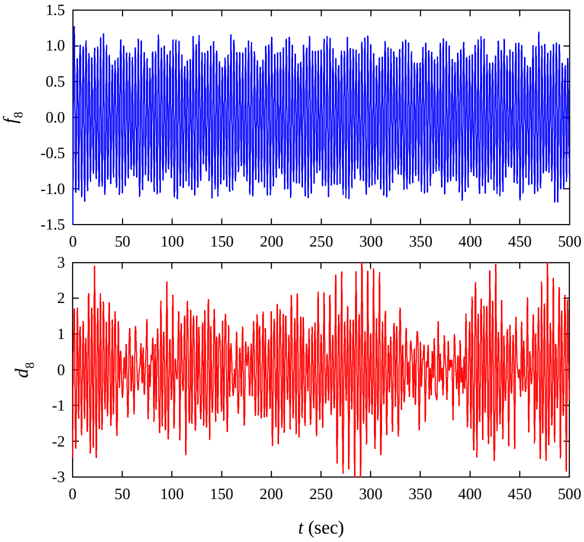

Figure 5 Example of chaotic-like time histories of riser (*f*) and wake (*d*) coordinates of a dominant 8th mode for ExxonMobil riser in linearly sheared current with V_{max} = 2.47 m/s

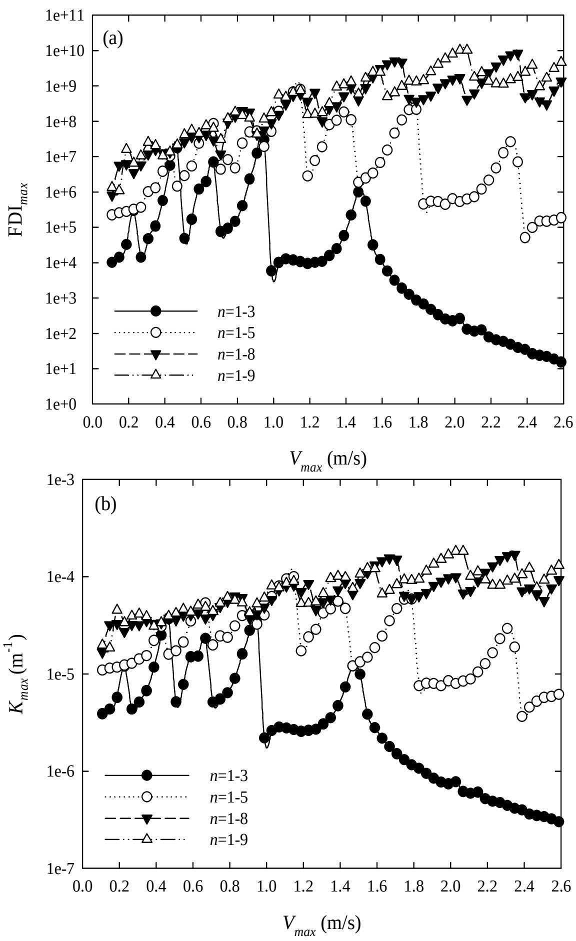

Figure 6 Variation of (a) FDI_{max} and (b) K_{max} with V_{max} for ExxonMobil riser in linearly sheared current

In some velocity cases, the time histories of some modal coordinates are non-periodic as opposed to the general lock-in condition where oscillating frequencies of riser and wake are nearly resonant or tuned as 1:1 ratio. This is exemplified in Fig. 5 where chaotic-like time traces of riser (*f*) and wake (*d*) coordinates corresponding to the dominant 8th mode are highlighted with V_{max}=2.47 m/s. It is seen that the wake response is more chaotic whereas the riser response is steadier.

The spatially maximum values of fatigue damage index (FDI_{max}) and RMS riser curvatures (K_{max}) are now evaluated (Eq. 19). They are displayed via the semi-log scale plots in Fig. 6 with varying V_{max} and *N*. It is seen that both Figs. 6a and 6b show similar features and trends with increasing *V*. The number of modes should be increased in the analysis since lower *N* model provides underestimated results at higher *V*. Both FDI_{max} and K_{max} increase with *V* when sufficient modes (*N* = 8 or 9) are accounted for.

4. NUMERICAL AND EXPERIMENTAL COMPARISONS

It is now interesting to make a comparison and discussion of numerical and experimental results for the predictions of riser VIV in uniform and sheared flows. The experimental post-processed results reported by Tognarelli *et al.* [9] are benchmarked and only cross-flow VIV are considered. Bare riser properties and parameters given in Table 1 have been chosen to match the experimented riser.

Figure 7 compares the values of $A_{rms,max}/D$ with varying *V* in the case of uniform flow. With respect to Figs. 2 and 3, nonlinear (NL) and linear (L) riser models are considered for *N* = 9. To show the effect of retained modes, results with *N* = 8 and 10 are also given. It can be seen that all models yield good agreement with experiment results in the low *V* range. For *V* > 0.8 m/s, the differences occur: the amplitudes numerically predicted by all *N* nonlinear models are lower than experimental amplitudes whereas those by linear model are still comparable, though being slightly lower, to the latter.

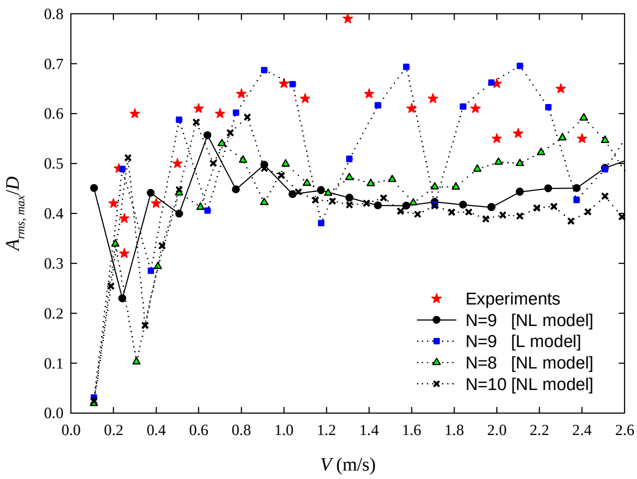

Figure 7 Comparison of $A_{rms,\,max}$ with varying *V* for ExxonMobil riser in uniform current: varying *N*

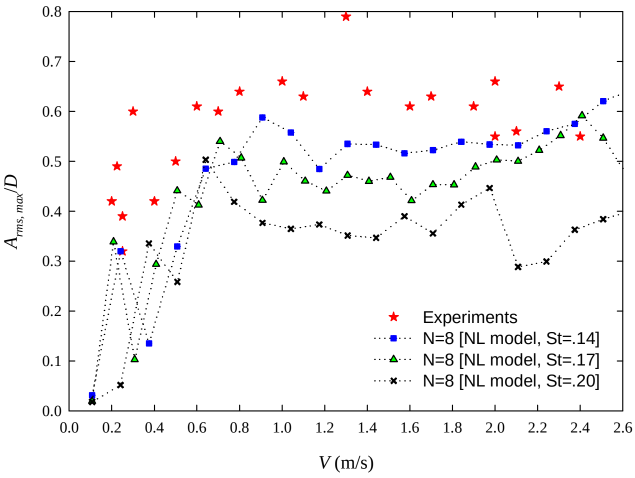

Figure 8 Comparison of $A_{rms,\ max}$ with varying V for ExxonMobil riser in uniform current: varying St

To show the influence of parameters, Fig. 8 compares the results with different St. In any case, the St value is fixed when varying V or Re number in the analysis. The effect of St is studied due to the fact that the reported St values were different in literature though post-processing the same ExxonMobil experimental data. That is, St = 0.21 in [9] whereas St = 0.14 in [20]. From Table 1, we consider the averaged value being 0.17. Because St has been incorporated into the theoretical model and governing formulae deriving wake coefficients, the predicted numerical results are influenced by St. This is shown in Fig. 8 where overall amplitudes decrease with increasing St.

Figure 9 plots the variation of FDI_{max} with varying V, corresponding to Fig. 7. It can be seen that numerical results are conservative when compared with experimented FDI_{max} values. However, all nonlinear models (N = 8, 9, 10) provide much better comparisons with experiment results than the linear model which considerably overestimates FDI_{max} as V increases. This over-prediction by linear riser model still exists in spite of increasing N as shown in Fig.10.

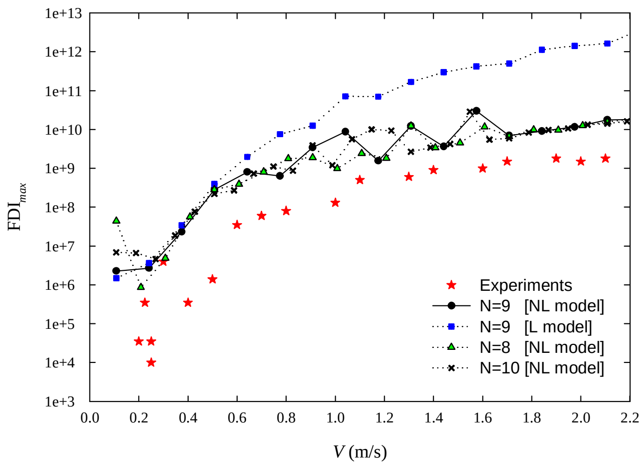

Figure 9 Comparison of FDI_{max} with varying V for ExxonMobil riser in uniform current: varying N

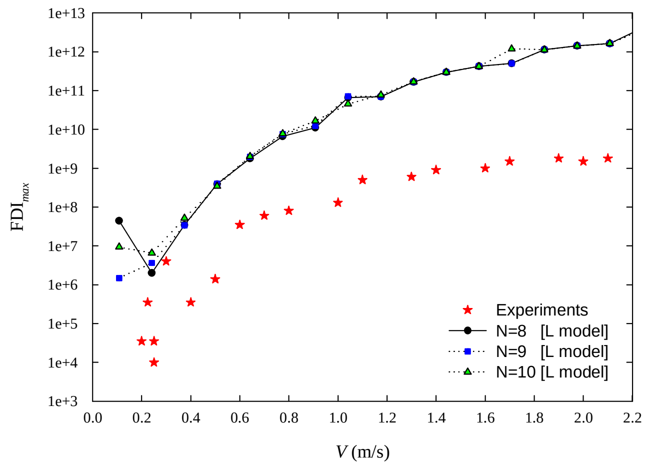

Figure 10 Comparison of FDI_{max} with varying V for ExxonMobil riser in uniform current: varying N for linear model

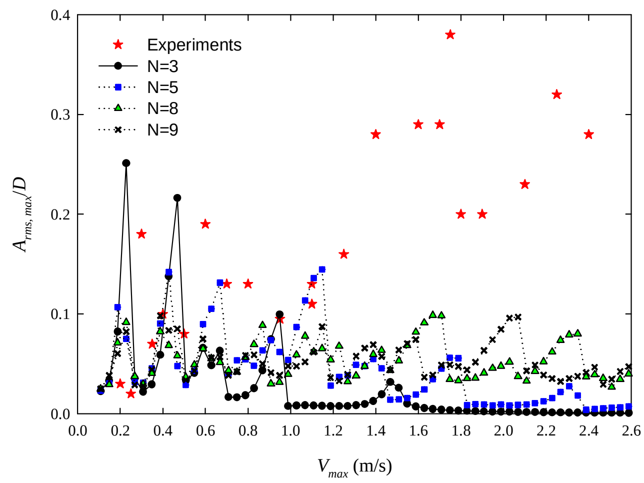

Figure 11 Comparison of $A_{rms,\ max}$ with varying V_{max} for ExxonMobil riser in sheared current: varying N for nonlinear model

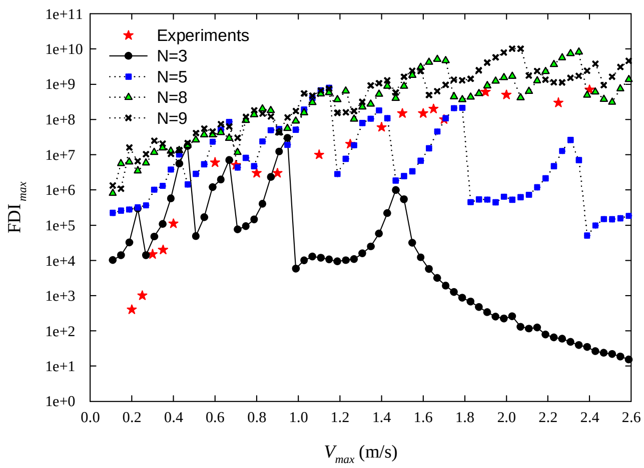

Figure 12 Comparison of FDI_{max} with varying V_{max} for ExxonMobil riser in sheared current: varying N for nonlinear model

In the sheared flow case, the numerical and experimental comparisons of $A_{rms,max}/D$ and FDI_{max} are displayed in Figs. 11 and 12, respectively. In Fig. 11, considerable discrepancies in response amplitudes are evident, even within numerical models with different N. The maximum $A_{rms,max}/D$ is about 0.38 by the experiments whereas it is less than 0.1, on average, by the numerical model (with N=8, 9). Nevertheless, the discrepancies between numerical and experimental results are decreased for the FDI_{max} plots in Fig. 12, like the case of uniform flow in Fig. 9. Overall, good comparisons of results are achieved when sufficient N modes are accounted for.

As a final remark, the effect of in-line motions – which has been neglected in this paper – should also be accounted for in the future theoretical model and analysis since coupled cross-flow/in-line VIV of risers are mostly realistic and they have been experimentally considered. Depending on overall system parameters and flow characteristics, the in-line motions would have an influence on both numerical result predictions and comparisons with experiments. The complete cross-flow/in-line VIV analysis would allow us to determine the real extent of the underlying effects of structural geometric nonlinearities and post-processing procedures.

5. CONCLUSIONS

A general reduced-order fluid-structure interaction model capable of evaluating the *multi-mode* nonlinear dynamics and interactions in marine risers subject to *uniform* and linearly *sheared* flows is presented. Cross-flow VIV due to fluctuating lift forces are considered and modeled through a *distributed* diffusive wake oscillator. The computational analysis is based on empirical coefficients, numerical integrations and time-domain simulations that robustly solve for few degrees of freedom governing displacement/velocity coordinates. When dealing with large parametric investigations, the system input parameters can be conveniently varied with some calibrations.

As far as the experimental benchmark is concerned, the ExxonMobil tested top-tensioned riser is considered in both the analysis and comparison. Some post-processed data have been reported in literature and herein referenced. Depending on the number of vortex-induced riser modes and their modal properties, the space-time varying amplitudes and displacement profiles are determined along with the bending strains and fatigue damage indices. Results highlight the effect of riser geometric nonlinearities on numerical VIV predictions, multi-mode interactions and numerical/experimental comparisons. This is qualitatively and quantitatively remarkable in the case of uniform flow which entails greater response amplitudes than the case of sheared flow.

In both uniform and sheared flow cases, a good qualitative comparison of fatigue damage indices is found between numerical and experimental results. This is plausible since bending strains have been directly measured and used in the fatigue approximations. This is in contrast to the experimented displacement amplitudes whose values have been typically obtained based on double integrations or a modal analysis in frequency domain with linear structural model. For this reason, a poorer comparison of riser amplitudes occurs and such the linear modal post-processing analysis has been questioned in some literature (e.g., [9]). Therefore, it is suggested relying on a comparison of bending strains or damage indices rather than response amplitudes. Overall, some quantitative errors are seen and these may be due to the wake oscillator’s inability to capture the actual flow physics in the wake and/or the experimental post-processing procedures.

To further validate and improve the presented theoretical reduced-order models and numerical results, the in-house experimental campaign will be established along with some CFD studies. These will provide new experimental benchmark which can improve our empirical wake oscillators. From a numerical standpoint, the travelling wave solution as well as direct numerical integrations of original nonlinear partial-differential equations of riser/wake could provide some new insightful aspects of sheared flow VIV such as the local lock-in due to cellular vortex shedding. These challenging issues are subject to future research investigations.

ACKNOWLEDGMENTS

The authors gratefully acknowledge the funding support from the Knowledge Transfer Partnerships (KTP) in the UK and would like to thank the reviewers for insightful comments which lead to the improvement of this paper.

REFERENCES

[1] Sumer, B. M, Fredsoe, J., 1997, *Hydrodynamics around Cylindrical Structures*, World Scientific, Singapore.

[2] Srinil, N., Wiercigroch, M., O'Brien, P., Younger, R., 2009, “Vortex-induced vibration of catenary riser: reduced-order modeling and lock-in analysis using wake oscillator”, in *Proc. The 28th OMAE*, Paper No.79166.

[3] Vandiver, J. K., Jaiswal, V., Jhingram, V., 2009, “Insights on vortex-induced, traveling waves on long risers”, *Journal of Fluids and Structures* **25**, 641-653.

[4] Govardhan, R. N., Williamson, C. H. K., 2006, “Defining the modified Griffin plot in vortex-induced vibration: revealing the effect of Reynolds number using controlled damping,” *Journal of Fluid Mechanics* **561**, 147-180.

[5] Miliou, A., Sherwin, S. J., Graham, J. M., 2003, “Fluid dynamic loading on curved riser pipes,” *Journal of Offshore Mechanics and Arctic Engineering* **125**, 176-182.

[6] Constantinides, Y., Oakley, O. H., 2009, “Numerical simulations of cylinder VIV focusing on high harmonics”, in *Proc. The 28th OMAE*, Paper No.80002.

[7] Chasparis, F., Modarres-Sadeghi, Y., Hover, F. S., Triantafyllou, M. S., Tognarelli, M., Beynet, P., 2009, “Lock-in, transient and chaotic response in riser VIV”, in *Proc. The 28th OMAE*, Paper No.79444.

[8] Chaplin, J. R., Bearman, P. W., Cheng, Y., Fontaine, E., Graham, J. M. R., Herfjord, K., Huera Huarte, F. J., Isherwood, M., Lambrakos, K., Larsen, C. M., Meneghini, J. R., Moe, G., Pattenden R. J., Triantafyllou, M. S., Willden, R. H. J., 2005. "Blind predictions of laboratory measurements of vortex-induced vibrations of a tension riser," *Journal of Fluids and Structures* **21**, 25-40.

[9] Tognarelli, M. A., Slocum, S. T., Frank, W. R., Campbell, R. B., 2004, "VIV response of a long flexible cylinder in uniform and linearly sheared currents", in *Proc. The OTC*, Paper No.16338.

[10] Constantinides, Y., Oakley, O. H., 2008, "Assessment of empirical VIV analysis tools and benchmark with experiments", in *Proc. The 27th OMAE*, Paper No.57216.

[11] Willden, R., Graham, J. M. R., 2004, "Multi-modal vortex-induced vibrations of a vertical riser pipe subject to a uniform current profile," *European Journal of Mechanics B/Fluids* **23**, 209-218.

[12] Gabbai, R. D., Benaroya, H., 2005, "An overview of modeling and experiments of vortex-induced vibration of circular cylinders," *Journal of Sound and Vibration* **282**, 575-616.

[13] Srinil, N., Wiercigroch, M., O'Brien, P., 2009, "Reduced-order modelling of vortex-induced vibration of catenary riser," *Ocean Engineering* **36**, 1404-1414.

[14] Vandiver, J. K., 1993, "Dimensionless parameters important to the prediction of VIV of long flexible cylinders in ocean currents", *Journal of Fluids and Structures* **7**, 423-455.

[15] Srinil, N., Rega, G., Chucheepsakul, S., 2007, "Two-to-one resonant multi-modal dynamics of horizontal/inclined cables. Part I: Theoretical formulation and model validation," *Nonlinear Dynamics* **48**, 231-252.

[16] Skop, R. A., Balasubramanian, S., 1997, "A new twist on an old model for vortex-excited vibrations," *Journal of Fluids and Structures* **11**, 395-412.

[17] Balasubramanian, S., Skop, R. A., Haan, F. L., A. A., Szewczyk, 2000, "Vortex-excited vibrations of uniform pivoted cylinders in uniform and shear flow", *Journal of Fluids and Structures* **14**, 65-85.

[18] Mathelin, L., de Langre, E., 2005, "Vortex-induced vibrations and waves under shear flow with a wake oscillator", *European Journal of Mechanics – B/Fluids* **24**, 478-490.

[19] Tognarelli, M. A., Taggart, S., Campbell, M., 2008, "Actual VIV fatigue response of full scale drilling risers: with and without suppression devices", in *Proc. The 27th OMAE*, Paper No.57046.

[20] Yang, G., Frank, W. R., Campbell, R. B., Slocum, S. T., 2008, "VIV model test data comparison with Shear7 V4.5," in Proceedings of the 27th OMAE, Estoril, Paper No.57108.

[21] Baarholm, G. S., Larsen, C. M., Lie, H., 2006, "On fatigue damage accumulation from in-line and cross-flow VIV on risers," *Journal of Fluids and Structures* **22**, 109-127.

[22] Vandiver, J. K., Allen, D., Li, L., 1996, "The occurrence of lock-in under highly sheared conditions", *Journal of Fluids and Structures* **10**, 555-561.